New Journal of Physics
The open-access journal for physics

Casimir–Lifshitz interaction between dielectric heterostructures

Arash Azari, Himadri S Samanta and Ramin Golestanian
Department of Physics and Astronomy, University of Sheffield, Sheffield S3 7RH, UK
E-mail: r.golestanian@sheffield.ac.uk

New Journal of Physics **11** (2009) 093023 (11pp)
Received 14 July 2009
Published 16 September 2009
Online at http://www.njp.org/
doi:10.1088/1367-2630/11/9/093023

Abstract. The interaction between arbitrary dielectric heterostructures is studied within the framework of a recently developed dielectric contrast perturbation theory. It is shown that periodically patterned dielectric or metallic structures lead to oscillatory lateral Casimir–Lifshitz forces, as well as modulations in the normal force as they are displaced with respect to one another. The strength of these oscillatory contributions increases with decreasing gap size and increasing contrast in the dielectric properties of the materials used in the heterostructures.

Contents

1. Introduction

In light of the ongoing miniaturization of mechanical devices and the recent developments in dispersion interactions [1]–[6], there has been some recent interest in the effect of these interactions between the components of small mechanical devices [7]. Since these interaction are particularly strong at small distances, it will be interesting to know how they can be utilized for designing novel mechanical systems that could work without physical contact and could potentially help solve the wear problem [8].

In the past few years, there has been a surge of interest in developing techniques that can be used to study the Casimir interaction in non-ideal geometries, including geometry perturbation theories [9]–[11], semiclassical [12] and classical ray optics [13] approximations, multiple scattering and multipole expansions [14]–[18], world-line [19] and quantum mechanical scattering [20] methods, exact numerical diagonalization methods [21, 22], field theoretical functional determinants method [23], as well as the numerical Green's function calculation method [24]. These methods have been used in studying the Casimir force in a variety of different geometries, which have improved significantly our understanding of the nontrivial geometry dependence of this effect.

The effect of non-ideal geometry has been shown to lead to a number interesting effects. For example, it has been suggested that corrugated surfaces opposite one another can experience an oscillatory lateral Casimir force [9], which was subsequently observed experimentally [5]. A recent experiment probing the normal Casimir force between a smooth surface and surface with tall rectangular corrugations also revealed further evidence on the non-additive nature of the Casimir force [6]. Moreover, there has also been recent progress in modulating the dielectric properties of the boundaries with the aim of controlling the Casimir force between them [27]. Here, we study the Casimir–Lifshitz interaction between arbitrary dielectric heterostructures within the framework of a recently developed formalism [25, 26]. We derive a closed form expression for the Casimir–Lifshitz energy between two dielectric heterostructures (such as the example depicted in figure 1) up to the second order in the perturbation theory and show that a coherent coupling between the different modes of the spectrum of the dielectric pattern takes place across the gap. As a special example, we consider unidirectional periodic heterostructures (see figure 1) and calculate the lateral and normal Casimir–Lifshitz force between them within the same order in the perturbation theory. We find that the coupling between modes with identical wavevectors of the pattern structures between the different objects can lead to modulations in the normal force and can give rise to oscillatory later forces, reminiscent of the lateral Casimir force that appears due to the coupling between geometrical features such as corrugations [5, 9].

This paper is organized as follows. Section 2 sketches the dielectric contrast perturbation theory, and section 3 elaborates on how it can be used for dielectric heterostructures giving closed form expressions for the second-order term in the perturbation theory. Section 4 gives the results for the lateral and normal Casimir–Lifshitz force for a number of choices of materials, and section 5 contains some discussions and concluding remarks.

2. Theoretical formulation

To calculate the Casimir–Lifshitz interaction we need to quantize the electromagnetic field in a background that includes the dielectric or metallic objects that modify the quantum fluctuations

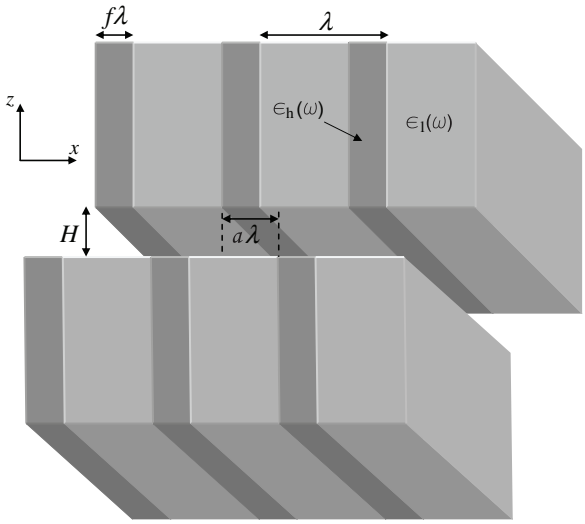

Figure 1. Schematic representation of two identical semi-infinite and periodic objects made of intercalated layers of *high* and *low* dielectric functions, occupying the fractions of f and $1-f$, respectively. Here H is the separation between them, a is a dimensionless lateral displacement, and λ is the wavelength of the periodic structure.

of the field. Describing a general assortment of dielectric and metallic objects in space via a frequency-dependent dielectric profile $\epsilon(\omega, \mathbf{r})$, we can write a general expression for the Casimir–Lifshitz energy as [26]

$$E = \hbar \int_0^\infty \frac{\mathrm{d}\zeta}{2\pi} \,\mathrm{tr}\, \ln\left[\mathcal{K}_{ij}(\zeta; \mathbf{r}, \mathbf{r}')\right], \tag{1}$$

where

$$\mathcal{K}_{ij} = \left[\frac{\zeta^2}{c^2}\epsilon(\mathrm{i}\zeta, \mathbf{r})\delta_{ij} + \partial_i\partial_j - \partial_k\partial_k\delta_{ij}\right]\delta^3(\mathbf{r}-\mathbf{r}'). \tag{2}$$

We can consider the dielectric function as $\epsilon(\mathrm{i}\zeta, \mathbf{r}) = 1 + \delta\epsilon(\mathrm{i}\zeta, \mathbf{r})$, and expand equation (1) in powers of the dielectric contrast. A similar approach has been the subject of a few recent studies [28]–[31].

The expansion leads to the decomposition of $\mathcal{K}_{ij}$ into a diagonal part $\mathcal{K}_{0,ij}$, corresponding to the empty space, and a perturbation part $\delta\mathcal{K}_{ij}$, namely

$$\mathcal{K}_{ij}(\zeta; \mathbf{q}, \mathbf{q}') = \mathcal{K}_{0,ij}(\zeta, \mathbf{q})(2\pi)^3\delta^3(\mathbf{q}+\mathbf{q}') + \delta\mathcal{K}_{ij}(\zeta; \mathbf{q}, \mathbf{q}'), \tag{3}$$

where

$$\mathcal{K}_{0,ij}(\zeta, \mathbf{q}) = \frac{\zeta^2}{c^2}\delta_{ij} + q^2\delta_{ij} - q_i q_j, \tag{4}$$

and

$$\delta\mathcal{K}_{ij}(\zeta; \mathbf{q}, \mathbf{q}') = \frac{\zeta^2}{c^2}\delta_{ij}\delta\tilde{\epsilon}(\mathrm{i}\zeta, \mathbf{q}+\mathbf{q}'). \tag{5}$$

This yields an expansion

$$\mathrm{tr}\ \ln[\mathcal{K}] = \mathrm{tr}\ \ln[\mathcal{K}_0] + \sum_{n=1}^{\infty} \frac{(-1)^{n-1}}{n}\,\mathrm{tr}[(\mathcal{K}_0^{-1}\delta\mathcal{K})^n], \tag{6}$$

where

$$\mathcal{K}^{-1}_{0,ij}(\zeta,\mathbf{q}) = \frac{\frac{\zeta^2}{c^2}\delta_{ij} + q_i q_j}{\frac{\zeta^2}{c^2}\left[\frac{\zeta^2}{c^2} + q^2\right]}. \tag{7}$$

The first term is the vacuum energy in the absence of the objects, and the terms in the series take account of their effect in a perturbative scheme. The nth-order term in equation (6) takes on the explicit form

$$\mathrm{tr}[(\mathcal{K}_0^{-1}\delta\mathcal{K})^n] = \int \frac{\mathrm{d}^3\mathbf{q}^{(1)}}{(2\pi)^3}\cdots\frac{\mathrm{d}^3\mathbf{q}^{(n)}}{(2\pi)^3}\frac{\left[\frac{\zeta^2}{c^2}\delta_{i_1 i_2} + q^{(1)}_{i_1}q^{(1)}_{i_2}\right]\cdots\left[\frac{\zeta^2}{c^2}\delta_{i_n i_1} + q^{(n)}_{i_n}q^{(n)}_{i_1}\right]}{\left[\frac{\zeta^2}{c^2} + q^{(1)2}\right]\cdots\left[\frac{\zeta^2}{c^2} + q^{(n)2}\right]}$$

$$\times\delta\tilde{\epsilon}(\mathrm{i}\zeta, -\mathbf{q}^{(1)} + \mathbf{q}^{(2)})\cdots\delta\tilde{\epsilon}(\mathrm{i}\zeta, -\mathbf{q}^{(n)} + \mathbf{q}^{(1)}), \tag{8}$$

which involves the Fourier transform of the dielectric contrast profile. Going to real space, we can rewrite the energy of the system as [26]

$$E = \hbar\int_0^{\infty}\frac{\mathrm{d}\zeta}{2\pi}\sum_{n=1}^{\infty}\frac{(-1)^{n-1}}{n}\int \mathrm{d}^3\mathbf{r}_1\cdots\mathrm{d}^3\mathbf{r}_n\mathcal{A}_{i_1 i_2}(\mathbf{r}_1-\mathbf{r}_2)\cdots\mathcal{A}_{i_n i_1}(\mathbf{r}_n-\mathbf{r}_1)$$

$$\times\left[\frac{\delta\epsilon(\mathrm{i}\zeta,\mathbf{r}_1)}{1+\frac{1}{3}\delta\epsilon(\mathrm{i}\zeta,\mathbf{r}_1)}\right]\cdots\left[\frac{\delta\epsilon(\mathrm{i}\zeta,\mathbf{r}_n)}{1+\frac{1}{3}\delta\epsilon(\mathrm{i}\zeta,\mathbf{r}_n)}\right], \tag{9}$$

where

$$\mathcal{A}_{ij}(\zeta,\mathbf{r}) = \frac{\zeta^2}{c^2}\frac{\mathrm{e}^{-\zeta r/c}}{4\pi r}\left[\delta_{ij}\left(1+\frac{c}{\zeta r}+\frac{c^2}{\zeta^2 r^2}\right) - \frac{r_i r_j}{r^2}\left(1+3\frac{c}{\zeta r}+3\frac{c^2}{\zeta^2 r^2}\right)\right], \tag{10}$$

We now use this formulation to study the Casimir–Lifshitz interaction between structures with inhomogeneous or patterned dielectric properties.

3. Dielectric heterostructures

Let us now consider a configuration similar to the one depicted in figure 1, namely two dielectric heterostructures that are placed parallel to each other at a separation H. Using the definition $\mathbf{r} = (\mathbf{x}, z)$, the dielectric profile can be written as

$$\epsilon(\mathrm{i}\zeta,\mathbf{r}) = \begin{cases} \epsilon_u(\mathrm{i}\zeta,\mathbf{x}), & \frac{H}{2} \leqslant z < +\infty, \\ 1, & \frac{-H}{2} < z < \frac{H}{2}, \\ \epsilon_{\mathrm{d}}(\mathrm{i}\zeta,\mathbf{x}), & -\infty < z \leqslant \frac{-H}{2}, \end{cases} \tag{11}$$

using the labels u and d for the 'up' and 'down' bodies, respectively.

To keep the calculations tractable, we now focus on the second-order term in the series expansion in equation (9). For such two semi-infinite bodies, the second-order interaction term

between the bodies can be written as

$$E_2 = -\frac{\hbar}{2\pi^2 c^2}\int_0^\infty \mathrm{d}\zeta\ \zeta^2 \int \mathrm{d}^2\mathbf{x}\mathrm{d}^2\mathbf{x}' \int \frac{\mathrm{d}^2\mathbf{Q}}{(2\pi)^2}\, \mathrm{e}^{\mathrm{i}\mathbf{Q}\cdot(\mathbf{x}-\mathbf{x}')}\, \mathcal{E}(Q) \left[\frac{\delta\epsilon_{\mathrm{u}}(\mathrm{i}\zeta,\mathbf{x})}{1+\frac{1}{3}\delta\epsilon_{\mathrm{u}}(\mathrm{i}\zeta,\mathbf{x})}\right]\left[\frac{\delta\epsilon_{\mathrm{d}}(\mathrm{i}\zeta,\mathbf{x}')}{1+\frac{1}{3}\delta\epsilon_{\mathrm{d}}(\mathrm{i}\zeta,\mathbf{x}')}\right], \tag{12}$$

for any lateral dielectric function profile, where

$$\mathcal{E}(Q) = \int_1^\infty \mathrm{d}p\ \frac{[2p^4-2p^2+1]}{\left[4p^2+(cQ/\zeta)^2\right]^{3/2}}\, \mathrm{e}^{(\zeta H/c)\sqrt{4p^2+(cQ/\zeta)^2}}, \tag{13}$$

and $\delta\epsilon_{\mathrm{u,d}}(\mathrm{i}\zeta,\mathbf{x}) = \epsilon_{\mathrm{u,d}}(\mathrm{i}\zeta,\mathbf{x}) - 1$.

We now focus on the specific example of the unidirectional periodic structures as depicted in figure 1, which is made of subsequent layers of materials with relatively *high* and *low* dielectric functions. We can use the periodic properties of the dielectrics and write them in the Fourier series expansion. As figure 1 shows, we can define the dielectric profile of the d-object as

$$\epsilon_{\mathrm{d}}(\mathrm{i}\zeta,x) = \begin{cases} \epsilon_{\mathrm{l}}(\mathrm{i}\zeta), & -\dfrac{\lambda}{2}+s\lambda \leqslant x \leqslant -\dfrac{f\lambda}{2}+s\lambda, \\ \epsilon_{\mathrm{h}}(\mathrm{i}\zeta), & -\dfrac{f\lambda}{2}+s\lambda < x < \dfrac{f\lambda}{2}+s\lambda, \\ \epsilon_{\mathrm{l}}(\mathrm{i}\zeta), & \dfrac{f\lambda}{2}+s\lambda \leqslant x \leqslant \dfrac{\lambda}{2}+s\lambda, \end{cases} \tag{14}$$

where s is an integer number. We define the Fourier series as

$$\frac{\delta\epsilon_{\mathrm{d}}(\mathrm{i}\zeta,x)}{1+\frac{1}{3}\delta\epsilon_{\mathrm{d}}(\mathrm{i}\zeta,x)} = \sum_{m=-\infty}^{\infty} \mathcal{C}_m(\mathrm{i}\zeta)\, \mathrm{e}^{\mathrm{i}2\pi mx/\lambda}, \tag{15}$$

where

$$\mathcal{C}_m(\mathrm{i}\zeta) = \frac{\sin m\pi f}{m\pi}\left[\frac{\delta\epsilon_{\mathrm{h}}(\mathrm{i}\zeta)}{1+\frac{1}{3}\delta\epsilon_{\mathrm{h}}(\mathrm{i}\zeta)} - \frac{\delta\epsilon_{\mathrm{l}}(\mathrm{i}\zeta)}{1+\frac{1}{3}\delta\epsilon_{\mathrm{l}}(\mathrm{i}\zeta)}\right] \tag{16}$$

for $m \neq 0$, and

$$\mathcal{C}_0(\mathrm{i}\zeta) = f\left[\frac{\delta\epsilon_{\mathrm{h}}(\mathrm{i}\zeta)}{1+\frac{1}{3}\delta\epsilon_{\mathrm{h}}(\mathrm{i}\zeta)}\right] + (1-f)\left[\frac{\delta\epsilon_{\mathrm{l}}(\mathrm{i}\zeta)}{1+\frac{1}{3}\delta\epsilon_{\mathrm{l}}(\mathrm{i}\zeta)}\right]. \tag{17}$$

We can find the corresponding expansion for the u-object by changing $x \to x + a\lambda$.

Using the Fourier series expansion, one can find the Casimir–Lifshitz energy between two dielectric heterostructures as depicted in figure 1 (up to second-order in the Clausius–Mossotti expansion of equation (9)) as

$$E_{\mathrm{pp}} = -\frac{\hbar A}{2\pi^2 c^2}{\sum_{m=0}^{\infty}}' \int_0^\infty \mathrm{d}\zeta\ \zeta^2 \mathcal{E}\left(\frac{2\pi m}{\lambda}\right) \mathcal{C}_m^2(\mathrm{i}\zeta)\cos(2\pi ma), \tag{18}$$

where the prime on the summation sign indicates that the $m = 0$ term is counted with half the weight, and the pp index means the energy calculated for the plate–plate geometry. This result shows that similar to the case of two corrugated surfaces, two patterned dielectric heterostructures also couple to each other at the leading order when the two wavelengths of

the modulations are equal [9]. Moreover, higher harmonics contribute to the Casimir–Lifshitz energy with exponentially decaying contributions, such that at large separations only the fundamental mode (lowest harmonic) will survive [21].

4. The normal and lateral forces

We now use equation (18) to calculate the normal and lateral forces between different types of dielectric and metallic heterostructures. We look at three different types of materials as examples, namely, gold, silicon and air/vacuum, and consider layered materials made of gold–silicon, silicon–air and gold–air. We describe the dielectric function of gold using a plasma model, namely, $\epsilon(\mathrm{i}\zeta) = 1 + \frac{\omega_\mathrm{p}^2}{\zeta^2}$, where ω_p is the plasma frequency, which is given as $\omega_\mathrm{p}(\mathrm{Au}) = 1.37 \times 10^{16}\,\mathrm{rad\,s^{-1}}$ [32]. For silicon, we use the Drude–Lorentz form $\epsilon(\mathrm{i}\zeta) = 1 + \frac{\omega_\mathrm{p}^2}{\zeta^2+\omega_0^2}$, where $\omega_\mathrm{p}(\mathrm{Si}) = 3.3\,\omega_0(\mathrm{Si})$ and $\omega_0(\mathrm{Si}) = 6.6 \times 10^{15}\,\mathrm{rad\,s^{-1}}$ [32]. Finally, for air/vacuum we use $\epsilon(\mathrm{i}\zeta) = 1$.

Due to difficulties in keeping the surfaces of the objects parallel to each other, most experiments are performed in plate–sphere geometry. To perform the calculation of the forces for the plate–sphere configuration, we can use the Derjaguin approximation [33], where we replace one of the semi-infinite objects with a planar surface with a sphere with radius R. The approximation is valid provided that the radius of sphere is much larger than the distance between the dielectric heterostructures as well as the wavelength of the dielectric heterogeneities, namely, $R \gg H\&\lambda$. Using this approximation, we can find the normal force between a semi-infinite dielectric heterostructure and a sphere of the same material composition as [33]

$$F_\mathrm{ps}^\mathrm{nor} = 2\pi R\left(\frac{E_\mathrm{pp}}{A}\right). \tag{19}$$

Using this result, we can find the Casimir–Lifshitz energy for the plate–sphere configuration as

$$E_\mathrm{ps} = -\int_H^\infty \mathrm{d}H'\, F_\mathrm{ps}^\mathrm{nor}(H'), \tag{20}$$

which we can now use to calculate the lateral Casimir force as

$$F_\mathrm{ps}^\mathrm{lat} = -\frac{1}{\lambda}\frac{\partial E_\mathrm{ps}}{\partial a}. \tag{21}$$

Substituting equations (19) and (20) into equation (21), it reads

$$F_\mathrm{ps}^\mathrm{lat} = \frac{2\pi R}{\lambda}\frac{\partial}{\partial a}\int_H^\infty \mathrm{d}H'\,\left(\frac{E_\mathrm{pp}(H')}{A}\right). \tag{22}$$

The above equations are the basis of the results that will be presented below.

Figures 2(a)–(c) show the normal Casimir–Lifshitz force between two unidirectional (layered) dielectric heterostructures as shown in figure 1 when laterally displaced with respect to one another by $a\lambda$. It corresponds to the symmetric case with $f = 0.5$, and the corrugation wavelength of $\lambda = 1\,\mu$m. Three different compositions of gold–silicon, silicon–air and gold–air are considered each at three different gap sizes of $H = 100$, 300 and 600 nm. The normal forces are normalized using the normal force F_ps^0 that corresponds to the Casimir–Lifshitz force calculated within the same scheme but with laterally averaged dielectric profile, which

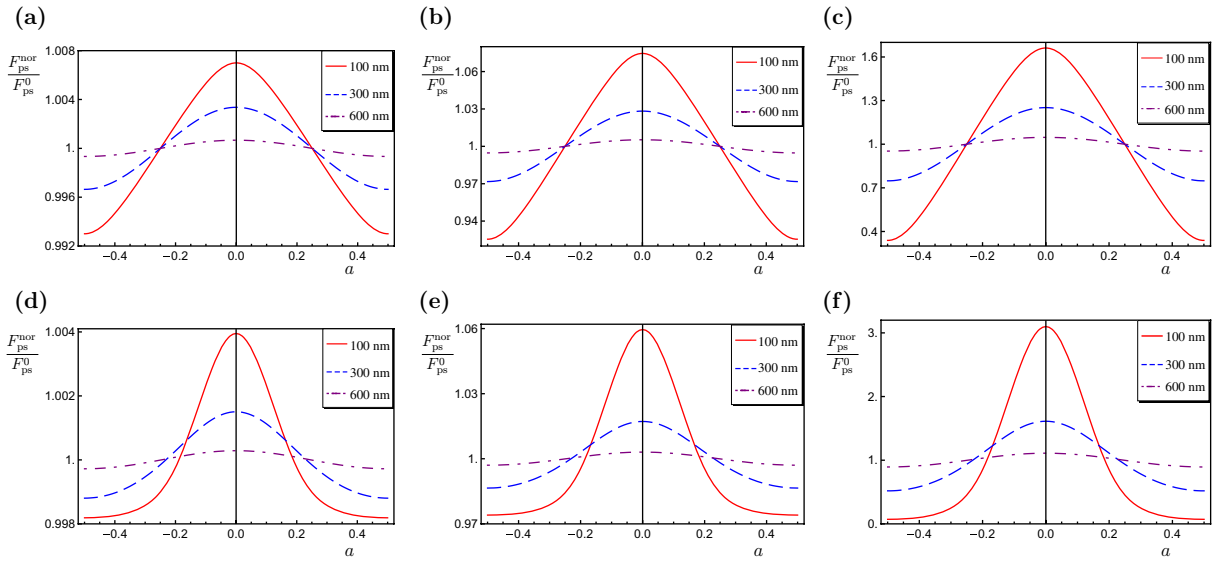

Figure 2. Normal Casimir–Lifshitz force between layered dielectric heterostructures as shown in figure 1 in the plate–sphere geometry, corresponding to (a) gold–silicon, (b) silicon–air and (c) gold–air, with $f = 0.5$, and to (d) gold–silicon, (e) silicon–air and (f) gold–air, with $f = 0.2$. The numerical value of corrugation wavelength used is $\lambda = 1\,\mu$m. Different curves correspond to different gap sizes of $H = 100$, 300 and 600 nm. The forces are normalized to $F_{\rm ps}^0$ that corresponds to the normal force when the laterally averaged dielectric profile is used.

corresponds to the $m = 0$ term in the expansion in equation (18). The normal force is found to oscillate as a function of the lateral displacement, having the maximum value when the regions of high dielectric constant from both sides are exactly opposite one another, and the minimum value when in the staggered configuration where regions of higher dielectric constant face regions of lower dielectric constant. The amplitude of the oscillations increases by decreasing the gap size, and the effect is progressively stronger when the contrast between the dielectric properties of the two regions is more pronounced, with a relative change of 0.7% for gold–silicon, 7% for silicon–air, and 65% for gold–air, at the closest separation of $H = 100$ nm.

In figures 2(d)–(f) the normal Casimir–Lifshitz forces between the same types of structures as above are presented, for the asymmetric case of $f = 0.2$. One can see two noticeable differences with the symmetric case. First, the oscillations are now asymmetric, as enforced by the asymmetry of the dielectric profile, although the asymmetry weakens as the gaps size increases and eventually disappears—i.e. the oscillations become symmetric and harmonic—at sufficiently large separations. This is consistent with the picture that different harmonics of the dielectric contrast profile in equation (18) couple with each other via an exponential terms that decays with the corresponding wavelengths of each harmonic and as a result any asymmetry caused by higher harmonics will die out at large gap sizes. The second new feature is the significant enhancement of the amplitude of the oscillatory behavior as a function of the lateral displacement, for the case of maximum contrast in the dielectric properties, namely, gold–air. While it is still the case that this amplitude increases with increasing contrast between

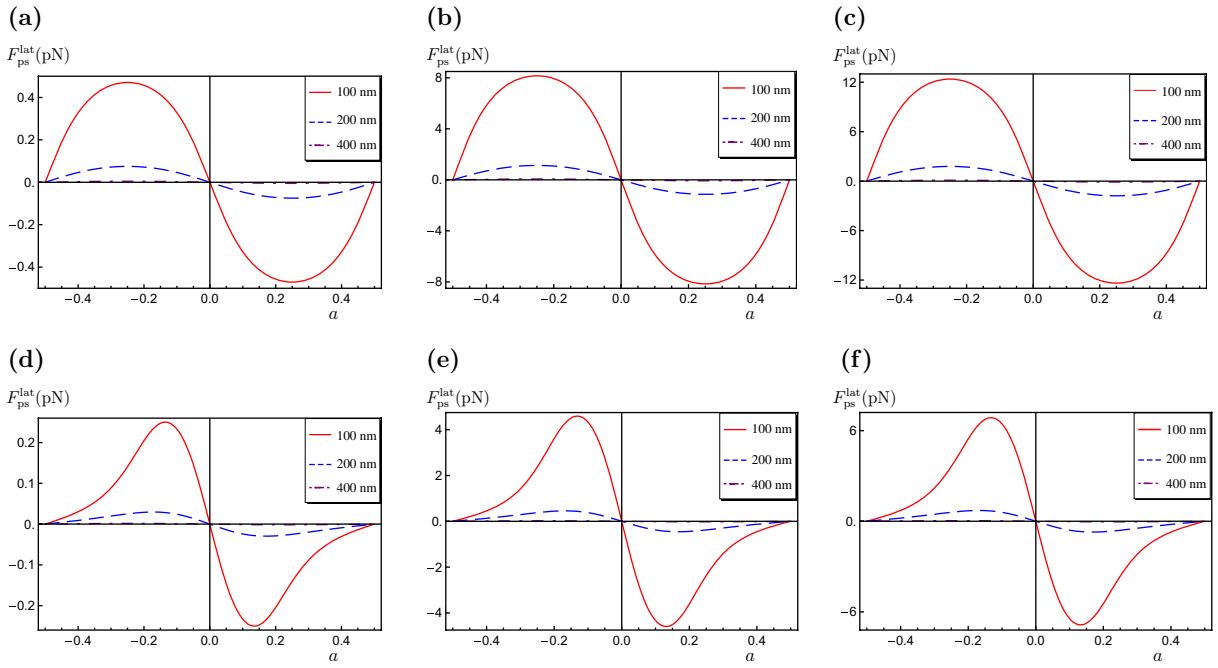

Figure 3. Lateral Casimir–Lifshitz force between layered dielectric heterostructures as shown in figure 1 in the plate–sphere geometry, corresponding to (a) gold–silicon, (b) silicon–air and (c) gold–air, with $f = 0.5$, and to (d) gold–silicon, (e) silicon–air and (f) gold–air, with $f = 0.2$. The numerical values used in these graphs are $\lambda = 1\,\mu$m and $R = 180\,\mu$m. Different curves correspond to different gap sizes of $H = 100$, 200 and 400 nm.

the dielectric properties of the two materials used in the layered structure, the relative change is 0.4% for gold–silicon, 6% for silicon–air and 200% for gold–air, at the closest separation of $H = 100$ nm.

The lateral Casimir–Lifshitz forces for the same layered structures as above are shown in figures 3(a)–(c) for the symmetric case with $f = 0.5$. In this case, we have assumed $R = 180\,\mu$m and $\lambda = 1\,\mu$m. Similar to the previous study, three different compositions of gold–silicon, silicon–air and gold–air are considered each at three different gap sizes of $H = 100$, 200 and 400 nm. The lateral force is found to oscillate as a function of the lateral displacement, reminiscent of the lateral Casimir force that is induced by geometrical corrugations [5, 9]. The shape of the oscillatory function approaches a sinusoidal behavior as the gap size increases, consistent with the fact that higher harmonics do not contribute to the force in that limit as also seen in the geometrical lateral Casimir effect [21]. The amplitude of the oscillations increases by decreasing the gap size as well as the contrast between the dielectric properties of the two regions. Numerically, we find an amplitude of 0.5 pN for gold–silicon, 8 pN for silicon–air and 12 pN for gold–air, at the closest separation of $H = 100$ nm.

Figures 3(d)–(f) show the lateral Casimir–Lifshitz forces between the same types of structures as above, for the asymmetric case of $f = 0.2$. Similarly, the profiles of the lateral force are noticeably asymmetric, with the asymmetry weakening as the gap size is increased and the shape of the profile approaches that of a sinusoidal function (single harmonic). A similar asymmetry also exists in the case of geometrical (corrugation-induced) lateral Casimir

force [5]. In contrast with the normal force, the lateral force is relatively much less sensitive to the contrast in the dielectric properties of the layers. The amplitude of the oscillations is found as 0.3 pN for gold–silicon, 5 pN for silicon–air and 7 pN for gold–air, at the closest separation of $H = 100$ nm.

5. Discussion

In this paper, we have proposed a mechanism by which it is possible to create a lateral Casimir–Lifshitz force as well as controlled modulations in the normal Casimir–Lifshitz force without geometrical corrugations. A coupling similar to what exists in the case of corrugated surfaces gives rise to these oscillatory forces, namely identical modes of the dielectric patterns couple across the gap to generate a macroscopic coherence in the fluctuations. The generic features of these oscillatory forces are very similar to those of the forces caused by corrugations; the effect is stronger and involves more harmonics at closer separations, while it weakens and only involves the lowest mode of the pattern in the dielectric contrast at larger separations.

While the difference in the dielectric properties of the materials controls the general strength of the above results, comparison between figures 2 and 3 shows that the modulations in the normal force are more strongly affected by the contrast in the dielectric properties. The choice of air/vacuum as one component also allows us to make predictions about geometrical features with large corrugation amplitudes, which provides an approximation scheme for the non-perturbative geometrical regime.

In the present calculations, we have only used the second-order terms in the dielectric contrast perturbative series. Higher order terms shown in equation (8) will introduce the coupling between different modes of the dielectric pattern in a systematic way, as imposed by the overall conservation of the sum of all wavevectors (momenta). While for the particular case studied here, the calculation of the higher order terms is not analytically tractable, we can shed some light on the potential effect of these terms by examining similar expansions in other cases. The issue of convergence of the dielectric contrast perturbation theory is discussed in [26], where it shown (based on the example of the exactly solvable system of semi-infinite flat dielectric objects) that the theory is convergent when the expansion parameter (that involves the dielectric function of the objects in the form of $\delta\epsilon/(1+\frac{1}{3}\delta\epsilon)$) at a characteristic imaginary frequency is roughly speaking smaller than 2. This, for example, means that while the theory is just about convergent in the case of silicon, it is strictly speaking not convergent for good conductors where the expansion parameter will reach the value of 3 at low frequencies. However, one can always rely on the leading order term to give the right order of magnitude and general behavior of the Casimir–Lifshitz interaction, and the higher order corrections in the dielectric contrast perturbation series—be they convergent or not—can in principle be summed up using standard techniques used in other asymptotic expansions in field theory such as the ϵ-expansion (Borel summation, etc). These correction will ultimately change the result in a quantitative, but not qualitative, manner. The present paper is aimed at showing the order of magnitude and generic features of the effect in terms of tractable calculations, for which the leading order term in the dielectric contrast perturbation is sufficient. We note that one can, in principle, carry out the calculation of the Casimir–Lifshitz interaction in such dielectric heterostructures using numerical diagonalization methods [21, 22], which will give numerically exact results.

The Derjaguin approximation for the calculation in the plate–sphere geometry is justified based on the general principle of the separation of length scales, and we note that its validity

in such structures has not been systematically investigated. We have chosen to represent our results in the plate–sphere geometry by using this approximation (as opposed to, for example, presenting them in the plate–plate geometry) in line of the main aim of the present paper which is to demonstrate the order of magnitude and the generic features of the forces in such heterostructures in realistic experimental situations.

Controlled interactions between dielectric heterostructures with smooth outer surfaces could be very useful in practical applications because it will help avoid the complications of bringing surfaces with geometrical protrusions close to each other while avoiding contact between them and controlling their separations. Moreover, it is much easier to pattern dielectric properties of materials in a controlled way than it is to shape them with the high precision that is needed for Casimir effect type experiments.

Acknowledgments

We thank the ESF Research Network CASIMIR for providing excellent opportunities for discussion on the Casimir effect and related topics. This work was supported by EPSRC under grant no. EP/E024076/1.

References

[1] Casimir H B G 1948 *Proc. Ned. K. Akad. Wet.* **51** 793
[2] Lifshitz E M 1956 *Sov. Phys. JETP* **2** 73
Dzyaloshinskii I E *et al* 1961 *Adv. Phys.* **10** 165
[3] Bordag M *et al* 2009 *Advances in the Casimir Effect* (Oxford: Oxford University Press)
[4] Lamoreaux S K 1997 *Phys. Rev. Lett.* **78** 5
Mohideen U and Roy A 1998 *Phys. Rev. Lett.* **81** 4549
Roy A and Mohideen U 1999 *Phys. Rev. Lett.* **82** 4380
Chan H B *et al* 2001 *Science* **291** 1941
Bressi G *et al* 2002 *Phys. Rev. Lett.* **88** 041804
Decca R S *et al* 2003 *Phys. Rev. Lett.* **91** 050402
Krause D E *et al* 2007 *Phys. Rev. Lett.* **98** 050403
Decca R S *et al* 2007 *Phys. Rev.* D **75** 077101
[5] Chen F *et al* 2002 *Phys. Rev. Lett.* **88** 101801
Chen F *et al* 2002 *Phys. Rev.* A **66** 032113
[6] Chan H B *et al* 2008 *Phys. Rev. Lett.* **101** 030401
[7] Serry F M *et al* 1995 *J. Microelectromech. Syst.* **4** 193
Buks E and Roukes M L 2001 *Phys. Rev.* B **63** 033402
Chan H B *et al* 2001 *Phys. Rev. Lett.* **87** 211801
Palasantzas G, De Hosson J and Th M 2005 *Phys. Rev.* B **72** 121409
[8] Ashourvan A *et al* 2007 *Phys. Rev. Lett.* **98** 140801
Ashourvan A *et al* 2007 *Phys. Rev.* E **75** 040103
Emig T 2007 *Phys. Rev. Lett.* **98** 160801
Miri M and Golestanian R 2008 *Appl. Phys. Lett.* **92** 113103
Lombardo F C *et al* 2008 *J. Phys. A: Gen. Math.* **41** 164009
Cavero-Peláez I *et al* 2008 *Phys. Rev.* D **78** 065019
[9] Golestanian R and Kardar M 1997 *Phys. Rev. Lett.* **78** 3421
Golestanian R and Kardar M 1998 *Phys. Rev.* A **58** 1713
Kardar M and Golestanian R 1999 *Rev. Mod. Phys.* **71** 1233

[10] Emig T *et al* 2001 *Phys. Rev. Lett.* **87** 260402
Emig T *et al* 2003 *Phys. Rev.* A **67** 022114
[11] Maia Neto P A *et al* 2005 *Phys. Rev.* A **72** 012115
Rodrigues R B *et al* 2006 *Phys. Rev. Lett.* **96** 100402
[12] Schaden M and Spruch L 1998 *Phys. Rev.* A **58** 935
[13] Jaffe R L and Scardicchio A 2004 *Phys. Rev. Lett.* **92** 070402
[14] Balian R and Duplantier B 1977 *Ann. Phys., NY* **104** 300
Balian R and Duplantier B 1978 *Ann. Phys., NY* **112** 165
[15] Kenneth O and Klich I 2006 *Phys. Rev. Lett.* **97** 160401
[16] Golestanian R 2000 *Phys. Rev.* E **62** 5242
[17] Emig T *et al* 2007 *Phys. Rev. Lett.* **99** 170403
[18] Emig T *et al* 2009 *Phys. Rev.* A **79** 054901
[19] Gies H and Klingmuller K 2006 *Phys. Rev. Lett.* **96** 220401
Gies H and Klingmuller K 2006 *Phys. Rev. Lett.* **97** 220405
[20] Bulgac A *et al* 2006 *Phys. Rev.* D **73** 025007
[21] Emig T 2003 *Europhys. Lett.* **62** 466
Büscher R and Emig T 2005 *Phys. Rev. Lett.* **94** 133901
[22] Lambrecht A and Marachevsky V N 2008 *Phys. Rev. Lett.* **101** 160403
[23] Bordag M 2007 *Phys. Rev.* D **75** 065003
[24] Rodriguez A *et al* 2007 *Phys. Rev. Lett.* **99** 080401
Rodriguez A *et al* 2007 *Phys. Rev.* A **76** 032106
Rodriguez A *et al* 2008 *Phys. Rev.* A **77** 062107
[25] Golestanian R 2005 *Phys. Rev. Lett.* **95** 230601
[26] Golestanian R 2009 *Phys. Rev.* A **80** 012519
[27] Chen F *et al* 2007 *Phys. Rev.* B **76** 035338
[28] Barton G 2001 *J. Phys. A: Gen. Math.* **34** 4083
[29] Buhmann S Y and Welsch D-G 2006 *Appl. Phys.* B **82** 189
[30] Veble G and Podgornik R 2007 *Eur. Phys. J.* E **23** 275279
[31] Milton K A, Parashar P and Wagner J 2008 *Phys. Rev. Lett.* **101** 160402
[32] Palik E D 1985 *Handbook of Optical Constants of Solids* ed E D Palik (New York: Academic)
[33] Israelachvili J N 1992 *Intermolecular and Surface Forces* (New York: Academic)